CrystEngComm

Accepted Manuscript

ROYAL SOCIETY OF CHEMISTRY

www.rsc.org/crystengcomm

Graphical abstract

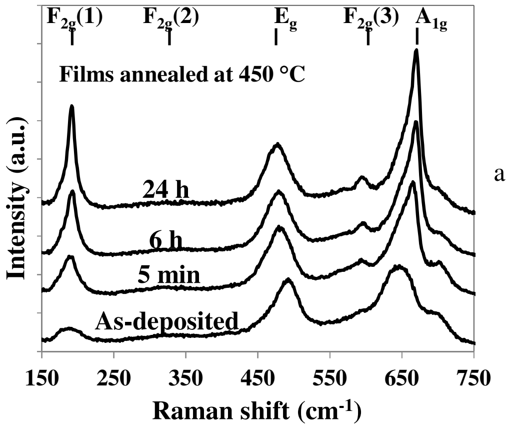

$Co_{1.7}Fe_{1.3}O_4$ thin films
are submitted to
a spinodal transformation
after annealing
at low temperature

Journal Name RSCPublishing

ARTICLE

Cite this: DOI: 10.1039/x0xx00000x

Received 00th January 2012,
Accepted 00th January 2012

DOI: 10.1039/x0xx00000x

www.rsc.org/

Thin films of $Co_{1.7}Fe_{1.3}O_4$ prepared by radio-frequency sputtering – First step towards their spinodal decomposition

T. M. A. Bui,[a,b,d] H. LeTrong,[a,b,c] L. Presmanes,[a,b] A. Barnabé,[a,b] C. Bonningue[a,b] and P. Tailhades*[a,b]

Pure thin films of $Co_{1.7}Fe_{1.3}O_4$ spinel iron cobaltites were prepared for the first time, by radio-frequency sputtering. Such films are made of small crystallites of about 20 to 30 nm in diameter. Because $Co_{1.7}Fe_{1.3}O_4$ films have a composition located in the miscibility gap of the Fe_3O_4-Co_3O_4, they can be submitted to a spinodal transformation below about 900 °C. This transformation was also confirmed at 600 °C by X-ray diffraction and transmission electron microscopy studies. It is demonstrated however that such a spinodal transformation occurs after only few hours at low temperature. Indeed, after an annealing in air at 300 to 450 °C for few hours, the spinodal transformation leading to two-phase spinels, one rich in iron and the other rich in cobalt, is clearly revealed by Raman spectroscopy and electrical measurements.

Introduction

A homogeneous solid solution led by cooling, inside a miscibility gap of a phase diagram, is not stable. It is progressively broken down into two different phases either by nucleation and growth or spinodal decomposition.[1] The first process can occur in the whole composition range of the miscibility gap and generally leads to random microstructures. The second one, which only operates in a limited area of the gap, can induce periodic microstructures at a submicronic scale. Such microstructures are particularly interesting when they contain at least a magnetic ordered phase. Giant magneto-resistance was thus observed in ferromagnetic alloys issued from spinodal decomposition.[2-4] Other collective properties could be obtained and used to make, for instance, magnonic crystals, the magnetic counterpart of photonic crystals.[5,6] The study of spinodal decomposition of magnetically ordered phases, could then be a key step in the quest for materials with original properties, likely to find new technological applications.

In the $CoFe_2O_4$-Co_3O_4 phase diagram,[7-11] there is a miscibility gap in which spinodal decomposition can lead to regular alternation of ordered magnetic phases made of iron-rich and cobalt-rich spinel oxides. However, this was mainly observed on powders.[9,12] Two works were about the preparation of thin films of iron cobaltites in this range of composition and the related spinodal decomposition.[11-12] Such films were obtained by the sol-gel process after annealing carried out above 800 °C. In the context of potential future applications, it is however necessary to be able to prepare thin films and to induce in them spinodal decomposition, at low temperatures. This work was then devoted to the preparation of thin films of iron cobaltites, by radio-frequency sputtering and to the study of the thermal behaviour of such films at moderate temperatures (< 500 °C).

$CoFe_2O_4$-Co_3O_4 phase diagram have already been established, experimentally[7-11] or from thermodynamic calculations.[14] These phase diagrams are very similar even if there are some discrepancies about the position and the area of the miscibility gap in which two spinel phases co-exist at the thermodynamical equilibrium. The global composition $Co_{1.7}Fe_{1.3}O_4$ is however close to the centreline of this region and to that of the more limited area, in which appears the spinodal decomposition. The composition $Co_{1.7}Fe_{1.3}O_4$ was then chosen for this work.

Experimental

Film preparation

Pure $Co_{1.7}Fe_{1.3}O_4$ was prepared by heating at 600 °C for 2 hours, a mixed oxalic precursor precipitated in a hydro-alcoholic medium. After adding a polyvinylic alcohol, the resulting powder was pressed inside a 100 mm in diameter matrix. The uniaxial pressure applied was 75 MPa. The green disc obtained was then slowly heated to eliminate the organic binder and then sintered at 900 °C for 12 hours. The relative density of the ceramic target thus prepared, was close to 60 %.

Thin films were prepared by radio-frequency (RF) sputtering of the previous ceramic target. The sputtering gas was pure argon and the apparatus was an Alcatel A450 equipped with a radio-frequency-generator (13.56 MHz) device as well as a pumping system (a mechanical pump coupled with a turbo molecular pump) which reaches residual pressures down to 10^{-5} Pa, a gas flow controller, a water cooled target holder and two water cooled sample holders. The films were deposited on silicon or glass substrates. Their thickness was 300 nm.

A residual vacuum close to 5×10^{-5} Pa was reached in the sputtering chamber before introducing the argon deposition gas. The target was sputtered for 20 hours at the beginning. The target was also sputtered for 10 minutes before each film deposition on the substrate. The sputtering conditions (RF power and argon pressure) have been optimized to obtain pure $Co_{1.7}Fe_{1.3}O_4$ spinel films.

Characterization

Structural characterizations of films were performed at room temperature by grazing angle X-ray diffraction (α=1 deg.) on a Siemens D5000 diffractometer equipped with a Brucker Sol-X detector. In situ high-temperature XRD data were collected in Bragg-Brentano θ-θ geometry using a Bruker D8 Advanced diffractometer equipped with an Anton Paar HTK 1200N heating chamber and a Bruker LynxEye position sensitive detector. XRD patterns were recorded under air every 50 °C from 50 to 900 °C with a data collection time of 20 min/scan and a 30 $°C\times min^{-1}$ heating rate. The films used for these experiments were 300 nm thick and deposited on pure silicon substrate because this material can withstand up to 900 °C despite a low oxidation of the surface not covered by the cobaltite. The X-ray wavelength was that of the copper Kα ray ($K_{\alpha1}$ = 0.15405 nm and $K_{\alpha2}$ = 0.15443 nm) for both diffractometers.

Imaging and elemental analyses were made using a JEOL 2100F field emission gun transmission electron microscope (FE-TEM) operating at 200 kV and equipped with an X-ray energy dispersive spectroscopy (X-EDS) system. X-EDS chemical composition mapping were also performed in scanning TEM (STEM) mode. For the cross-section TEM and STEM observations, the thin films were deposited on silicon substrate, cut into thin slices normal to the interfaces which were glued together between spacers and finally ion milled to perforation.

Raman spectra were collected under ambient conditions using a Labraham HR 800 Jobin Yvon spectrometer with 633 cm^{-1} Ar^+ ion laser. Spectra acquisition was carried out for 400 seconds using an x100 objective lens and 600 gr/mm grating. During the measurement, the resulting laser power at the surface of the sample was adjusted to 0.7 mW. Examination of multiple spots showed that the samples were homogeneous. The substrate chosen was a quartz microscope slide able to be heated up to 600 °C without damage. Unlike silicon, this substrate has no Raman signal in the spectral range analysed.

The magnetic properties were measured in the plane of the films, with a vibrating sample magnetometer Versalab Free from Quantum Design. The maximal applied field for the measurements was 30 k.Oe. The magnetization of the samples was corrected for substrate contribution.

Film thicknesses were measured using a Dektak 3030ST mechanical profilometer. Atomic force microscopy (AFM) was carried out with a Veeco Dimension 3000 atomic force microscope. The microstructure of the samples was also investigated by scanning electron microscopy with a JEOL JSM 6700F apparatus.

Results and discussion

As-deposited films

The nature of the phases obtained after RF sputtering, depends on the preparation conditions. The RF power density has a strong influence, as it is revealed by figure 1. For a RF power close to 40 W and an argon pressure of 0.5 Pa, the film is made of a mixed cobalt iron monoxide. This phase seems pure because all the diffraction peaks can be ascribed to the XRD pattern of cobalt-iron monoxide. Moreover, the magnetization (M) versus magnetic field (H) do not displays hysteresis curve that could reveal an extra ferrimagnetic spinel phase. When the RF power density is decreased, the X-ray diffraction pattern of a spinel phase replaces the previous pattern (Fig. 1). Some changes in (220) peaks intensity are observed for samples containing little monoxide. These changes cannot be attributed to changes in cationic distributions because the very small difference in electronic density of the Co^{2+}, Co^{3+} and Fe^{3+} ions, cannot produce such large variations in XRD peaks intensity. The reason for these changes seems rather related to a crystallite growth in a preferred direction.

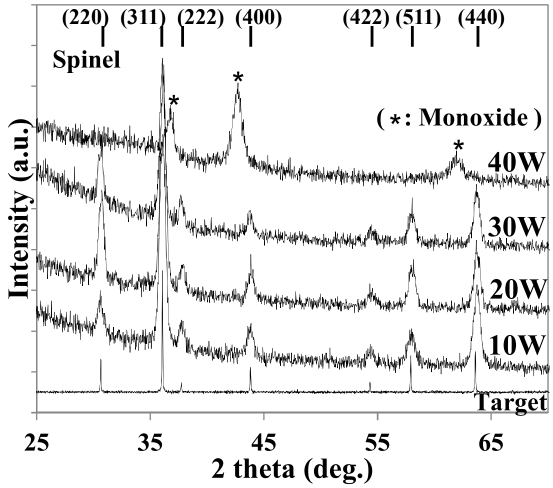

Fig. 1 X-ray diffraction patterns of films deposited at 0.5 Pa argon pressure for different RF powers.

The M=f(H) curves are clearly hysteresis curves for these samples as shown in Fig. 2 for the film deposited at 20 W. The coercive force is very high at 150 K (close to 12 kOe) but decreases down to 3.6 kOe at room temperature. This behaviour, due to a high magnetocrystalline anisotropy strongly dependent to temperature, is similar to that observed by Takahashi and Fine.[15] A slightly lower magnetization at 30 kOe is observed for the film prepared at 30 W. This magnetization is only 72.8 emu/cm^3 while it is nearby 82.6 and 86.4 emu/cm^3 for the films prepared at 20 and 10 W respectively. This could be explained by the presence of a small quantity of monoxide, which does not contribute as strongly to the magnetization of the film, than the ferrimagnetic spinel phase.

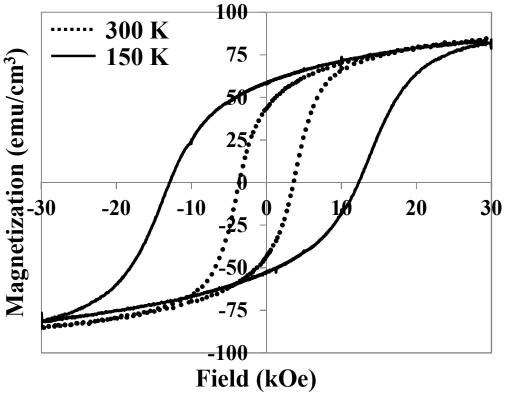

Fig. 2 Hysteresis loop registered at 150 K and 300 K of films deposited at 0.5 Pa - 20 W.

Some experiments carried out at argon pressures increasing from 0.5 to 1.5 Pa, show also that this modification of sputtering conditions leads to a decrease in magnetization measured at 30 kOe. Moreover, for the higher argon pressures, the X-ray diffraction patterns reveal the formation of the monoxide in addition to the spinel phase.

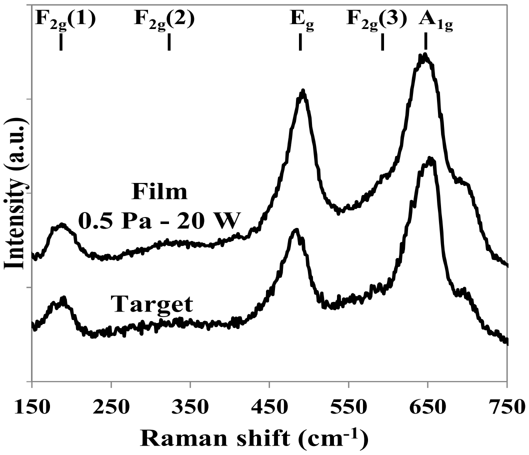

Fig. 3 Raman spectra of films deposited at 0.5 Pa-20W.

When the argon pressure and the RF power density are fixed to 0.5 Pa and 20 W respectively, the films obtained display the X-ray diffraction pattern of a pure spinel phase and have a high magnetization. They also display the same Raman spectrum as a pure $Co_{1.7}Fe_{1.3}O_4$ spinel powder (Fig. 3). Similar results were obtained for 0.5 Pa and 10 W but the deposition rate is lower in this case. The sputtering conditions selected for the preparation of the samples studied in the following part, dedicated to the study of the thermal stability of the films, were then 0.5 Pa and 20 W. The microstructure of such films is made of small columns well crystalized of about 20 to 30 nm in diameter (Fig. 4). The Ra roughness of the films, measured by atomic force microscopy, is close to 2 nm.

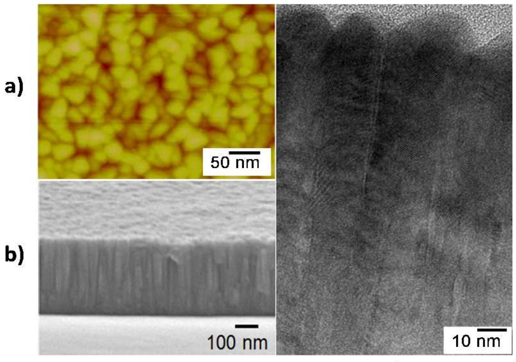

Fig. 4 Microstructure of films deposited at 0.5 Pa - 20 W: AFM planar view (4a), SEM (4b) and TEM (4c) cross sec-tion view.

Annealed films

As it was pointed out in introduction, the $Co_xFe_{3-x}O_4$ solid solutions got so far, at about 900 to 950 °C and then quenched to room temperature, are not stable in the miscibility gap (from RT to about 875 °C). The $Co_{1.7}Fe_{1.3}O_4$ RF-sputtered films of this work, were not treated at such temperatures because the sputtering process of oxides generally leads to temperatures lower than 200 °C on the substrate surface. However, due to thermodynamic reasons, they have also to be transformed in the miscibility gap even if different parameters, such as mechanical stress, crystallite size, could influence the mechanism and the speed of transformation observed for samples studied so far. Their thermal stability inside the miscibility gap was then carefully studied, mainly at quite low temperatures compatible with the use of ordinary glass substrates.

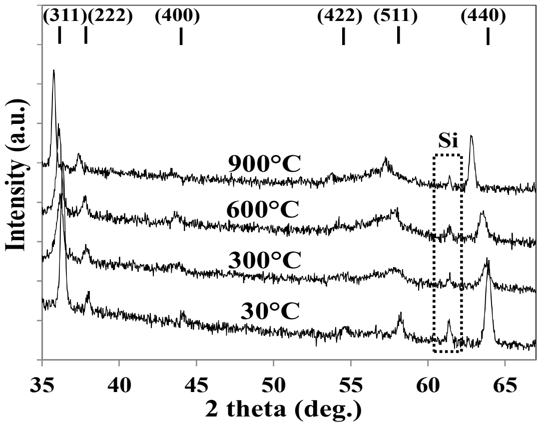

Fig. 5 XRD patterns registered at different temperatures for films deposited at 0.5 Pa - 20 W.

The first experiments were carried out in an X-ray diffractometer equipped with a heating chamber. Figure 5 shows that the peaks corresponding to the spinel structure are not clearly modified by these heating conditions apart from a slight shift of the Bragg position towards low 2 theta angles due to the thermal expansion. However, a broadening of peaks is found for the powder diffraction pattern recorded at 700 °C. Some other diffractograms were recorded at 600 °C for different durations (Fig. 6). Above about 5 hours of hold time, some peaks start to split (i.e. (440) for instance). This split indicates that the initial single phased film is transformed into two spinel phases. An iron-rich phase and another rich in cobalt, with crystalline parameters respectively greater and smaller than the initial phase, are growing progressively according to the characteristic process of the spinodal decomposition.[11] After cooling to room temperature, the sample remains two-phased.

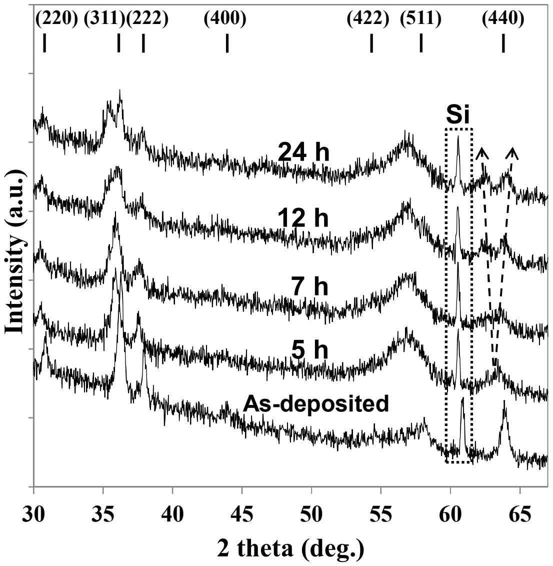

Fig. 6 XRD patterns registered at 600 °C for films deposited at 0.5 Pa - 20 W on silicon substrate.

The structural changes of $Co_{1.7}Fe_{1.3}O_4$ films were also studied by Raman spectroscopy. The $Co_{1.7}Fe_{1.3}O_4$ film deposited on quartz was heated in a conventional furnace at 600 °C for increasing durations. Raman spectra reveal the main peaks related to the spinel oxides, already identified in previous works.[16-18] They are also changing with the duration of heat treatment (Fig. 7). The main changes, especially for above 6 hours, are the very strong growth of the $F_{2g}(1)$ and A_{1g} peaks. The emergence of low-intensity $F_{2g}(2)$ and $F_{2g}(3)$ peaks must also be reported. X-ray diffraction shows that the spinodal decomposition is only pointed out after more than 5 hours of treatment. This is in good accordance with XRD analysis which shows that the spinodal decomposition is only pointed out after more than 5 hours of treatment.

To understand such changes, it is interesting to have a look on the Raman spectra of cobalt-rich ($Co_{2.46}Fe_{0.54}O_4$) and iron-rich ($Co_{1.22}Fe_{1.78}O_4$) spinel powder as reference samples (Fig. 7).

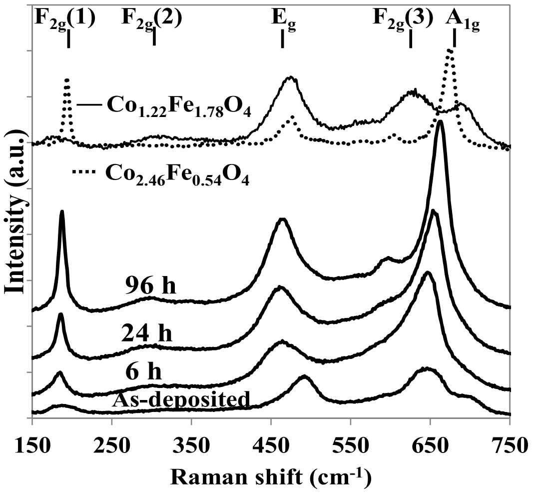

Fig. 7 Raman spectra of films deposited at 0.5 Pa - 20 W annealed at 600 °C for different annealing times. Comparison with Raman spectra of $Co_{1.22}Fe_{1.78}O_4$ (iron rich spinel) and $Co_{2.46}Fe_{0.54}O_4$ (cobalt rich spinel).

These powders have chemical compositions very close to those ($Co_{2.69}Fe_{0.31}O_4$ and $Co_{1.16}Fe_{1.84}O_4$) obtained after complete transformation of the $Co_{1.7}Fe_{1.3}O_4$ cobaltite.[19] In other words, they have very similar compositions of those given by the lateral branches of the miscibility gap at low temperature. The Raman spectra of these powders are quite different. Very well defined $F_{2g}(1)$ and A_{1g} peaks and, in a less extend, $F_{2g}(1)$ peak, are observed for the co-rich phase. This can be ascribed to a high content of Co^{2+} ions in tetrahedral sites ($F_{2g}(1)$ peak) and to a high content of Co^{3+} ions in octahedral sites (A_{1g} peak). According to [19] the structural formula of the co-rich phase is indeed:

$$Co_1^{2+}[Co_{1.46}^{3+}Fe_{0.54}^{3+}]O_4^{2-} \quad \text{(formula 1)}$$

(cations outside and inside brackets are located in tetrahedral and octahedral sites respectively). By contrast, a small $F_{2g}(2)$ peak is characteristic of the iron-rich phase. It is then clear that the superposition of such spectra, leads to a spectrum similar to that observed after a long heat treatment of the $Co_{1.7}Fe_{1.3}O_4$ film. The growth of the $F_{2g}(1)$ and A_{1g} peaks and the emergence of low-intensity $F_{2g}(2)$ and $F_{2g}(3)$ peaks after heat treatments, are so simply explained by the formation of cobalt-rich and iron rich phases.

According to previous results,[19] the transformation of $Co_{1.7}Fe_{1.3}O_4$ powders by spinodal or nucleation and growth, does not lead to a strong difference in the average coordinence of each cation in the spinel lattices of the material. The real change is that the cations are located in two separated phases in such a manner that some cations are "concentrated" in a sub-lattice in a given spinel phase. For instance, the formation of a cobalt-rich phase leads to a rate of about 100 % of Co^{2+} ions and 75 % of Co^{3+} ions in its tetrahedral and octahedral sub-lattices respectively (see formula 1). The contribution to the Raman spectra of such a phase, which is significantly different than that of an iron-rich phase in which cobalt ions are "diluted" in the two sub-lattices, thus becomes clearly visible.

Raman spectroscopy is then very sensitive to the formation of a new spinel phase very rich in cobalt ions.

No clear contrast between the two phases formed by spinodal transformation at 600 °C for 24 hours, was highlighted. Local chemical analyses were also unable to reveal the phases individually as shown by the homogeneous distribution of the iron and cobalt species in the cross section STEM view (Fig. 8a). A complete segregation occurs however, after a much longer annealing time. For instance, a sample heat treated in air at 600 °C for 96 hours, clearly displays cobalt rich and iron rich regions of about 50 nm in diameter (Fig. 8b). The random distribution of the two phases in these regions along and perpendicular to the columns, reveals however that the spinodal transformation is replaced by a nucleation and growth process for such a very long time of treatment at 600 °C.

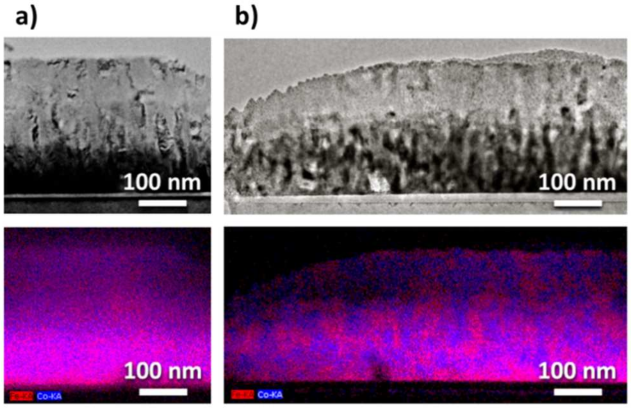

Fig. 8 Cross section STEM micrographs and corre-sponding EDS maps obtained at iron (red) and cobalt (blue) Kα for the films annealed at 600 °C for 24 h (8a) and 96 h (8b).

In order to achieve spinodal decomposition at moderate temperature, annealing treatment at 450 °C were also carried out. The annealing of the films at 450 °C, increases a little bit the average grain size. Indeed, atomic force microscopy reveals that the mean diameter of the grains, changes from 30 to about 50 nm. After 24 hours of treatment at 450 °C, there is no clear change in X-ray diffraction patterns. A careful examination of the pattern, shows however a very little broadening of the peaks. This is in contradiction with the increase of the size of the grains. Coarser grains would suggest an improvement of crystallization, revealed by narrower diffraction peaks. The peak broadening could then reveal the beginning of the spinodal decomposition.

The Raman spectroscopy is however more informative (Fig. 9). After only 5 minutes of treatment at 450 °C, the $F_{2g}(1)$ and A_{1g} peaks, but also $F_{2g}(3)$, grow significantly in a manner similar to that observed for films decomposed at 600 °C. This growth continues for longer annealing times. It seems then reasonable to conclude that the spinodal decomposition starts after few minutes when the $Co_{1.7}Fe_{1.3}O_4$ is heated at 450 °C, even if no clear change in X-ray diffraction pattern is observed. The changes observed trough Raman spectroscopy, could be the first step of spinodal decomposition already described by Harrison and Putnis,[20] which corresponds to the development of low-amplitude sinusoidal fluctuation of compositions. The gathering of cobalt ions in small region could make possible its detection by Raman spectroscopy, but the gradual variation of the composition induced by this first step of the spinodal decomposition, could make difficult the characterization by X-ray diffraction. Just a small peak broadening could just be expected from this technique.

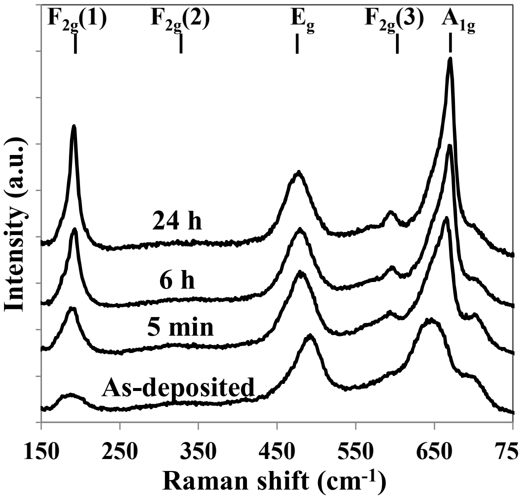

Fig. 9 Raman spectra of films deposited at 0.5 Pa - 20 W annealed at 450 °C for several times.

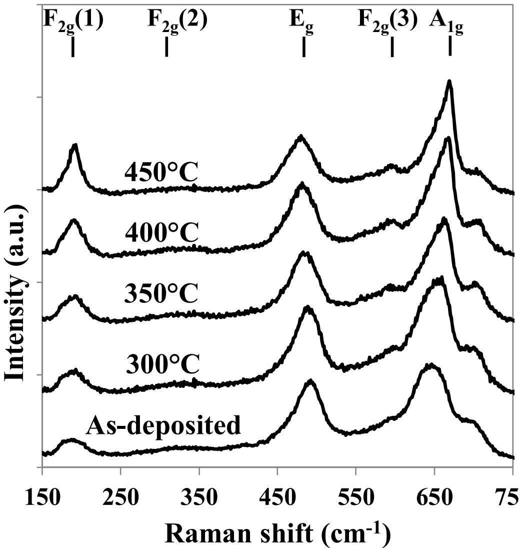

Fig. 10 Raman spectra of films deposited at 0.5 Pa-20W annealed for 2h at different temperatures.

Treatments at temperatures even lower than 450 °C, were also carried out. It was very surprising to see that after only 2 hours at 300 °C, the Raman spectrum of $Co_{1.7}Fe_{1.3}O_4$ film begins to move towards the shape of decomposed cobaltites spectra (Fig. 10). This evolution is obviously more pronounced for treatments at higher temperatures. Fig. 11 clearly illustrates the initiation of decomposition for mild heating and its progress for more energetic treatments. The $F_{2g}(1)$ peak intensity, normalized by that of Eg peak, which remains approximately constant along the treatments, grows regularly and significantly with the heating temperature and time.

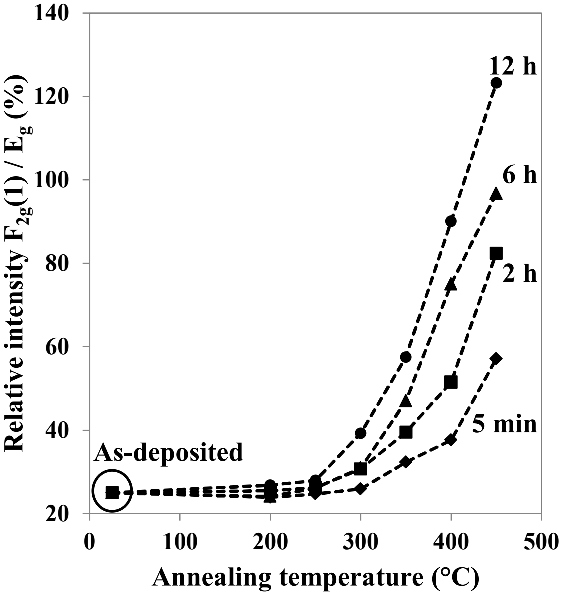

Fig. 11 The evolution of $F_{2g}(1)$ Raman peak relative intensity for films deposited at 0.5 Pa - 20 W versus annealing temperature and time.

Electron exchanges between M^{n+} and $M^{(n+1)+}$ cations located in the same sub-lattice, induce semi-conducting properties in spinel oxides.[21] $Co_{1.7}Fe_{1.3}O_4$ is thus a semiconductor because its structural formula is close to:

$$Co^{2+}_{0.61}Fe^{3+}_{0.39}[Co^{2+}_{0.39}Co^{3+}_{0.73}Fe^{3+}_{0.88}]O^{2-}_{4} \quad \text{(formula 2)}$$

according to.[19] However, due to the high activation energy of the electronic exchange for the Co^{2+}/Co^{3+} couples,[22,23] the electrical resistivity of such a material is quite high at room temperature, but decreases strongly at higher temperatures. The electrical resistivities of the as-sputtered and heat treated $Co_{1.7}Fe_{1.3}O_4$ samples, were then studied at 250 °C, to make the measurements possible with our experimental set-up. A quite high activation energy, close to 0.48 eV, was measured in agreement with the bibliographical data.[22,23] On the other hand, figure 12 shows that the resistivity of the films increases almost linearly with the time of annealing at 450 °C. That clearly demonstrates significant changes in the material at this moderate temperature of treatment. According to[19] at the end of the transformation of $Co_{1.7}Fe_{1.3}O_4$ in the miscibility gap, the cobalt-rich phase formed is an insulator because it has no more Co^{2+} and Co^{3+} ions on the same sub-lattice. The iron-rich phase ($Co_{1.16}Fe_{1.84}O_4$), which is also created, is however a semiconductor. But, its structural formula close to:

$$Co^{2+}_{0.30}Fe^{3+}_{0.70}[Co^{2+}_{0.70}Co^{3+}_{1.16}Fe^{3+}_{1.14}]O^{2-}_{4} \quad \text{(formula 3)}$$

shows that the number of Co^{2+}/Co^{3+} couples is much lower than that of the initial single phase $Co_{1.7}Fe_{1.3}O_4$ (see structural formula 2). The spinodal decomposition of this latter necessarily leads to a progressive increase in resistivity. This is in agreement with the results of the electrical measurements shown in Fig. 12. The combination of the results coming from Raman spectroscopy and electrical measurements seem then to prove the beginning of the spinodal transformation, after heat treatments at very moderate temperatures for quite short time of annealing.

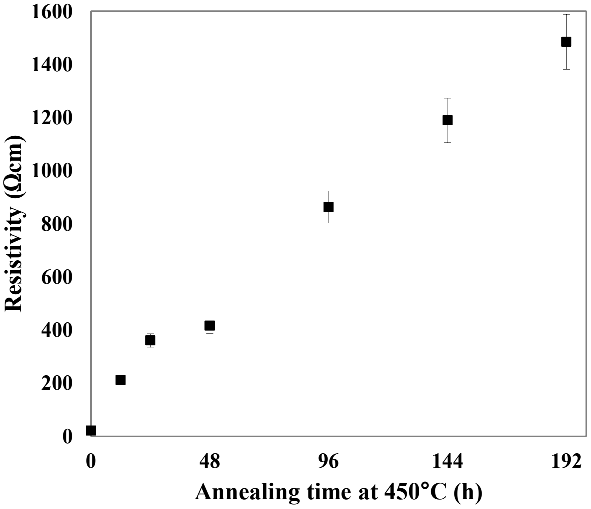

Fig. 12 Electrical measurement at 250 °C of films deposited at 0.5 Pa - 20 W annealed at 450 °C for different durations.

Conclusion

Thin films of $Co_{1.7}Fe_{1.3}O_4$ were prepared for the first time, by RF sputtering on substrate at room temperature. Pure as-deposited samples are made of small crystallites of about few tens of nanometers. Because they have a composition inside the miscibility gap of the phase diagram of $CoFe_2O_4$-Co_3O_4, their thermal stability were studied. It was shown that $Co_{1.7}Fe_{1.3}O_4$ films are not stable at 600 °C as for cobaltites of similar composition, already prepared at high temperature in the form of powders or thin films. More original results were obtained however. It was demonstrated using mainly Raman spectroscopy and electrical measurements, that $Co_{1.7}Fe_{1.3}O_4$ films can be partially transformed at quite low temperatures, lying from 300 to 450 °C, and after quite short time of annealing. This partial transformation is a first step of spinodal decomposition. From the present work it can then be conclude that the preparation of thin films structured by spinodal transformation, could be obtained at temperatures compatible with the use of cheap substrate as conventional glass slides or silicon wafers.

Acknowledgements

Thi Mai Anh Bui wishes to thank the Vietnamese Government Scholarship (Project 322) of Vietnam Ministry of Education and Training and the support of Carnot Institute CIRIMAT for her Ph.D grant.

Notes and references

[a] Université de Toulouse; UPS-INPT; Institut Carnot CIRIMAT; 118 route de Narbonne, F-31062 Toulouse cedex 9, France. E-mail : tailhade@chimie.ups-tlse.fr; Fax: 33 (0)5 61 55 61 63 ; Tel: 33 (0)5 61 55 61 74
[b] CNRS; Institut Carnot Cirimat; F-31062 Toulouse cedex 9, France.
[c] Ho Chi Minh city University of Science, Vietnam National University, 227 Nguyen Van Cu Q5 - 750000 Ho Chi Minh city, Viet Nam.
[d] University of Transport and Communications, Lang Thuong – Dong Da – Ha Noi - Viet Nam.

1 J.W. Cahn and J.E. Hilliard, *J. Chem. Phys*., 1958, **28**, 258-267.
2 M.G.M. Miranda, E. Esteves-Rams, G. Martinez and M.N. Baibich, *Phys. Rev. B*, 2003, 68, 01443.
3 M.G.M. Miranda, A.T. da Rosa, R. Hinrichs, U. Golla-Schindler, A.B. Antunes, G. Martinez, E. Esteves-Rams and M.N. Baibich, *Physica B*, 2006, **384**, 175-178.
4 A. Hutten, D. Sudfeld, K. Wojcrykowski, P. Jutzi and G. Reiss, *J. Mag. Mag. Mat*., 2003, **262**, 23-31.
5 S.A. Nikitov, Ph. Tailhades and C.S. Tsai, *J. Mag. Mag. Mat*., 2001, 236, 320-330.
6 Yu V. Gulyaev, S.A. Nikitov, L.V. Zhivotovskii, A.A. Klimov, Ph. Tailhades, L. Presmanes, C. Bonningue, C.S. Tsai, S.L. Vysotskii and Y.A. Filimonov, *JETP Lett.*, 2003, **77**, 567-570.
7 J. Robin, *Ann. Chim (Paris)*, 1955, **10**, 389-412.
8 M. Takahashi and M.E. Fine, *J. Am. Ceram. Soc*., 1970, **53**, 633-634.
9 M. Takahashi, J.R.C. Guimares and M.E Fine, *J. Am. Ceram. Soc*., 1971, **54**, 291-295.
10 P.J. Murray and J.W. Linnett, *J. Phys. Chem. Solids*, 1976, **37**, 619-624.
11 S. Hirano, T. Yogo, K. Kikuta, E. Asai, K. Sugiyama and H. Yamamoto, *J. Am. Ceram. Soc*., 1993, **76**, 1788-1792.
12 K.J. Kim, J.H. Lee and C.S Kim, *J. Korean Phys. Soc*., 2012, **61**, 1274-1278.
13 H. Le Trong, A. Barnabé, L. Presmanes and Ph. Tailhades, *Solid State Sci.*, 2008, **10**, 550-556.
14 I-H Jung, S. Decterov, A.D. Pelton, H-M Kim, Y-B Kang, *Acta Materialia*, 2004, **52**, 507-519.
15 M. Takahashi and M.E. Fine, *J. Appl. Phys*., 1972, **43**, 4205-4216.
16 H. Shirai, Y. Morioka and I. Nakagawa, *J. Phys. Soc. Jpn*., 1982, **51**, 592-597.
17 V.G Hadjiev, M.N. Iliev and I.V. Vergilov, *J. Phys. C*., 1988, **21**, 199-201.
18 P. Chandramohan, M.P. Srinivasan, S. Velmurugan and S.V. Narashimhan, *J. Solid State Chem*., 2011, **184**, 89-96.
19 H. Le Trong, L. Presmanes, E. De Grave, A. Barnabé, C. Bonningue, Ph. Tailhades, *J. Mag. Mag. Mat*., 2013, **334**, 66-73.
20 R.J. Harrison and A. Putnis, *Surv. Geophys*., 1999, **19**, 461-520.
21 E.J.W. Verwey, and P.W. Haayman, *Physica*, 1941, **8**, 979-987.
22 G.H. Jonker, *J. Phys. Chem. Solids*, 1959, **9**, 165.
23 P.A. Cox "Electronic structure and chemistry of solids", *Oxford Science Publications*, 1987, 184.